The Optical Gravitational Lensing Experiment. Miras and Semiregular Variables in the Large Magellanic Cloud*

I. S o s z y ń s k i[1,2], A. U d a l s k i[1], M. K u b i a k[1], M.K. S z y m a ń s k i[1], G. P i e t r z y ń s k i[1,2], K. Ż e b r u ń[1], O. S z e w c z y k[1], Ł. W y r z y k o w s k i[1], and K. U l a c z y k[1]

[1]Warsaw University Observatory, Al. Ujazdowskie 4, 00-478 Warszawa, Poland
e-mail:
(soszynsk,udalski,mk,msz,pietrzyn,zebrun,szewczyk,wyrzykow,kulaczyk)@astrouw.edu.pl
[2] Universidad de Concepción, Departamento de Fisica, Casilla 160–C, Concepción, Chile

ABSTRACT

We use the OGLE-II and OGLE-III data in conjunction with the 2MASS near-infrared (NIR) photometry to identify and study Miras and Semiregular Variables (SRVs) in the Large Magellanic Cloud. We found in total 3221 variables of both types, populating two of the series of NIR period–luminosity (*PL*) sequences. The majority of these objects are double periodic pulsators, with periods belonging to both *PL* ridges. We indicate that in the period – Wesenheit index plane the oxygen-rich and carbon-rich AGB stars from the NIR *PL* sequences C, C′ and D split into well separated ridges. Thus, we discover an effective method of distinguishing between O-rich and C-rich Miras, SRVs and stars with Long Secondary Periods using their *V* and *I*-band photometry. We present an empirical method of estimating the mean K_s magnitudes of the Long Period Variables using single-epoch K_s measurements and complete light curves in the *I*-band. We utilize these corrected magnitudes to show that the O-rich and C-rich Miras and SRVs follow somewhat different K_s-band *PL* relations.

Stars: AGB and post-AGB – Stars: late-type – Stars: oscillations – Magellanic Clouds

1. Introduction

Our knowledge of the Long Period Variables (LPVs) significantly increased when large microlensing surveys collected large enough amount of photometric data to reliably determine the periods and other parameters of these stars. Wood *et al.* (1999) showed five parallel sequences in the period–luminosity (*PL*) plane (labeled A–E), each populated by LPVs of different features. As a luminosity in the *PL* diagram Wood *et al.* (1999) used reddening free Wesenheit index, but

*Based on observations obtained with the 1.3 m Warsaw telescope at the Las Campanas Observatory of the Carnegie Institution of Washington.

very similar picture was shown for the near-infrared (NIR) K waveband (Wood 2000). Earlier two of these sequences were known: *PL* relation for Miras (Glass and Lloyd Evans 1981) and the additional sequence for Semiregular Variables (SRVs, Wood and Sebo 1996).

The subsequent papers confirmed and extended these results (Cioni *et al.* 2001, Noda *et al.* 2002, Lebzelter *et al.* 2002, Cioni *et al.* 2003). Important progress in this field has been made due to the analysis of the photometric data originated in the Optical Gravitational Lensing Experiment (OGLE) conjuncted with the NIR measurements from various sources (2MASS, SIRIUS, DENIS). The OGLE project is a large scale photometric survey regularly monitoring the densest regions of the sky. Collected long-term photometric data of millions of objects are an ideal material for studying a wide variety of variable stars, also red giants.

Kiss and Bedding (2003) used OGLE and 2MASS data to show that the Wood's sequence B above the Tip of the Red Giant Branch (TRGB) is made up with two sequences. Moreover, below the TRGB there are three sequences which are shifted in $\log P$ relative to the *PL* relations above the TRGB. This was the final proof that the majority of the pulsating variables below the TRGB are the first ascent giants (RGB stars). These results were confirmed by Ita *et al.* (2004), who labeled by C′ the new discovered sequence between the sequences B and C. We adopt this notation in this paper.

Soszyński *et al.* (2004a) showed the complex structure of the *PL* distribution analyzing the OGLE Small Amplitude Red Giants (OSARGs) – stars which most frequently can be found in the sequences A and B. When the secondary periodicities of these multi-periodic variables are taken into consideration, one can find that these objects lie in the four relatively narrow *PL* sequences. Moreover, Soszyński *et al.* (2004a) empirically showed that the variables fainter than the TRGB are a mixture of the AGB and RGB stars and both groups follow different *PL* relations. Finally, to complicate this pattern, it was shown that the ridge A below the TRGB consist of three closely spaced parallel sequences, what is distinctly visible in the Petersen diagram of these variables.

The aim of the present study is to show that the structure of the sequences C′, C and D is also more complex than it looked at the first glance. We discovered that each of these sequences splits into two ridges in the period – optical Wesenheit index plane. These division corresponds to the spectral separation into oxygen-rich and carbon-rich AGB stars. We use this feature to separate both spectral types of variables, and show that O-rich and C-rich Miras and SRVs follow somewhat different *PL* relations in the K_s waveband.

The paper is organized as follows. In Section 2 we describe the I and V-band observations and the cross-correlation of the optical and NIR data. In Section 3 we present the selection of the Miras and SRVs in our data. Section 4 describes the sample and some features of the *PL* relations are presented. In Section 5 we show period – optical Wesenheit index diagram on which the O- and C-rich AGB stars are well separated. Section 6 contains the description of the mean K_s-band magnitudes estimation. In Section 7 we present *PL(K)* diagram for Miras and SRVs. Our results are discussed and summarized in Sections 8 and 9.

2. Observations and Data Reductions

The optical data used in this analysis were obtained from the 1.3 m Warsaw Telescope at the Las Campanas Observatory, Chile, operated by the Carnegie Institution of Washington. The *I*-band data span a time baseline of about 3000 days: from January 1997 to April 2005. During the years 1997–2000, when the second phase of the OGLE survey (OGLE-II) was conducted, the telescope was equipped with the "first generation" camera with the SITe 2048×2048 CCD detector. The pixel size was 24 μm what corresponded to 0.417 arcsec/pixel scale. Observations of the LMC were performed in the "slow" reading mode of the CCD detector with the gain 3.8 e^-/ADU and readout noise of about 5.4 e^-. Details of the instrumentation setup can be found in Udalski, Kubiak and Szymański (1997).

Since 2001, when the third stage of the project (OGLE-III) started, the telescope has been equipped with a "second generation" eight chip 8192×8192 pixel CCD mosaic camera (Udalski 2003). The pixel size of the detector is 15 μm, giving the 0.26 arcsec/pixel scale and the field of view about $35' \times 35'$. The gain of each chip is adjusted to be about 1.3 e^-/ADU with the readout noise from 6 to 9 e^- depending on the chip.

V-band measurements were collected during the second phase of the OGLE experiment, so they span shorter time baseline. Up to 70 *V*-band points per star is available. In the *I*-band we collected in total from 500 to 900 measurements, depending on the field. The observations were reduced with the Difference Image Analysis developed by Alard and Lupton (1998) and Alard (2000), implemented by Woźniak (2000) and Udalski (2003). The transformations of the instrumental photometry to the standard system, and the determination of the equatorial coordinates of stars is described by Udalski *et al.* (2000).

The NIR K_s and J measurements used in this work come from the 2MASS All-Sky Catalog of Point Sources (Cutri *et al.* 2003). We performed the spatial cross-correlation of the OGLE variables with the 2MASS catalog in two steps. In the first step for each OGLE star we found the closest object in the 2MASS list. Then, for each OGLE field we determined the mean offset between OGLE and 2MASS positions. The typical value of the offset was equal to 0.5 arcsec in RAcos(δ) and 0.1 arcsec in DEC. In the second step of the procedure we shifted the 2MASS positions by the offsets and repeated the cross-identification of objects using the 1 arcsec search radius. That way we successfully identified more than 98% of the OGLE red stars ($V-I>0.5$ mag) brighter than $I=17$ mag.

For further analysis we included only sources detected in four photometric band-passes: V, I, J and K_s, and stars with $V-I>0.5$ mag. The data have been dereddened using the extinction maps provided by Udalski *et al.* (1999) with the extinction law by Schlegel *et al.* (1998).

3. Selection of the Sample

We performed a period search in the same manner as described by Soszyński *et al.* (2004a). Briefly, we used period-searching program FNPEAKS (Kołaczkowski 2003, private communication) which implements the algorithm of Discrete Fourier Transform. We tested periodicity of every I-band light curve brighter than 17 mag. After finding the highest peak in the power spectrum, we fitted the third order Fourier series to the folded light curve and subtracted the function from the data. Then, we repeated the procedure using the residuals until we found five periods per star. During the search we determined the I-band amplitudes for each period by deriving the difference between the maximum and minimum values of the fitted function.

We identified Miras and SRVs in the LMC using two features: I-band amplitudes and position in the period – NIR Wesenheit index diagram. The Wesenheit index (Madore 1982) is a reddening-free quantity defined as a linear combination of the selected luminosity and color of the star:

$$W_{\lambda_1\lambda_2} = m_{\lambda_2} - R_{\lambda_1\lambda_2}(m_{\lambda_1} - m_{\lambda_2})$$

where $R_{\lambda_1\lambda_2}$ is the ratio of total-to-selective absorption at given wavebands:

$$R_{\lambda_1\lambda_2} = \frac{A_{\lambda_2}}{E(\lambda_1 - \lambda_2)} = \frac{R_{\lambda_2}}{R_{\lambda_2} - R_{\lambda_1}},$$

$$R_\lambda = \frac{A_\lambda}{E(B-V)}.$$

Usually the optical magnitudes and colors are utilized to construct this quantity, for example:

$$W_{VI} \equiv W_I = I - 1.55(V-I).$$

However, the Wesenheit index can be defined also for the NIR data, for example K_s-band magnitudes and $(J-K_s)$ colors. Having Schlegel's *et al.* (1998) ratios of total-to-selective absorption ($R_J = 0.902$, $R_K = 0.367$) we obtained the following definition of the NIR Wesenheit index:

$$W_{JK} = K_s - 0.686(J - K_s).$$

Fig. 1 shows the period–W_{JK} diagram for red giants in the LMC. The PL sequences are better defined than in the K_s-band PL diagram, in particular when the random-phase single-epoch measurements are plotted. We used amplitudes and a position in the $\log P$–W_{JK} diagram to identify our sample of Miras and SRVs.

Before selecting the stars populating the sequence C we excluded variables with amplitudes smaller than 0.1 mag. In the case of the sequence C′ we cut the sample at $A(I) = 0.03$ mag. We checked that below these limits these sequences are not visible among real or artificial small amplitude variables (see also Groenewegen 2004).

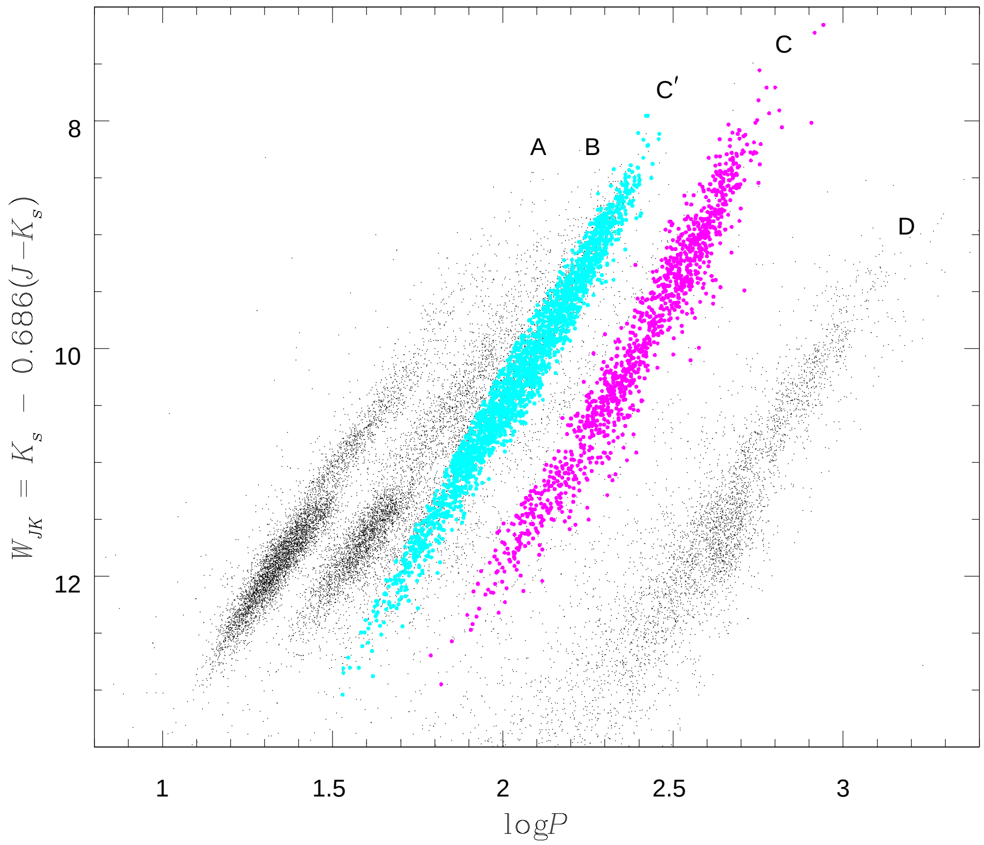

Fig. 1. Period–W_{JK} diagram for Miras and SRVs in the LMC. The sequences C′ and C are highlighted in cyan and magenta, respectively.

Then, we selected LPVs from the sequences C and C′ using their position in the $\log P$–W_{JK} diagram (Fig. 1). Because each star in Fig. 1 is represented by a single-epoch observation in K_s and J-bands, we employed the rule that the larger the amplitude of variability, the larger possible deviation from the mean *PL* law. In the final step of our procedure all selected light curves were carefully checked visually. Obvious eclipsing and ellipsoidal variables, foreground high proper motion stars, artifacts etc. were removed from the sample.

It is worth noting that an additional dim sequence is visible between sequences C′ and C. It is built by rather small amplitude variables (0.02 mag$<A(I)<0.2$ mag). The same sequence is noticeable in Fraser *et al.* (2005) (their Fig. 1).

4. Miras and Semiregular Variables

We selected 1112 variables with the primary period in the sequence C and 2109 objects populating sequence C′. This division is in many cases ambiguous, because multiperiodicity is a common feature among these stars. About half of the stars populating the sequence C and about 70% of objects with dominant periods in the sequence C′ have one of the secondary periods obeying the other *PL* relation. Sometimes the amplitudes of both modes are similar, and the determination of the main periods could be different, if somewhat different set of data is used.

The list of all variables is available in the electronic form from the OGLE INTERNET archive:

http://ogle.astrouw.edu.pl/
ftp://ftp.astrouw.edu.pl/ogle/ogle2/var_stars/lmc/lpv/

or its US mirror

http://bulge.princeton.edu/~ogle/
ftp://bulge.princeton.edu/ogle/ogle2/var_stars/lmc/lpv/

We provide the equatorial coordinates, primary periods, V, I, J and K_s magnitudes, amplitudes and classification of the stars. Individual *BVI* measurements of all objects and finding charts are also available from the OGLE INTERNET archive. The lists contain together 3586 entries but only 3221 objects, because 365 stars were detected twice – in the overlapping regions of adjacent fields.

The sequences C and C′ spread down to the luminosities more than 1 mag below the TRGB. However, we do not find any bump in the luminosity function below the TRGB, as it was visible for the OSARG variables (Ita *et al.* 2002, Kiss and Bedding 2003). This likely means that the sequences C and C′ are composed solely with the AGB stars.

Practically all Miras, *i.e.*, variables with $A(V) > 2.5$ mag (Kholopov *et al.* 1985) or $A(I) > 0.9$ mag, fall on the sequence C. The remaining stars in this ridge are formally SRVs, because their amplitudes do not fulfill these arbitrary criteria. Nevertheless, we did not find any distinct boundary between Miras and SRVs and the sequence C, what suggests that these stars represent the same type of variables. To the end of this paper we will call them "Mira-like variables".

There are strong arguments that the sequences C and C′ represent fundamental and first overtone modes of pulsation, respectively, although this question is not settled yet. Wood *et al.* (1999) suggested that the next sequences (B and A, *i.e.*, the OSARG variables) are populated by the next successive modes: the second and higher overtones. This idea was shared by many other authors, although the theoretical *PL* relations do not fit the observed sequences (Ita *et al.* 2004, Fraser *et al.* 2005). Soszyński *et al.* (2004a) showed that there are important empirical arguments that OSARGs are different types of pulsating stars, and they are not the higher overtones of Miras and SRVs. The analysis of the secondary periodicities of these variables showed that OSARGs populate four narrow *PL* sequences, different than sequences C′ and C. Moreover, the *PL* sequence A and B (and other OSARG's sequences) are roughly parallel to the sequences C and C′ in the $\log P$–K diagram, but these ridges have different slopes in the $\log P$–W_I plane. The sequence B even crosses the sequence C′ in the period–W_I diagram at brighter magnitudes. Of course, the *PL* relations formed by the successive overtones should have the same relative positions on each type of the *PL* diagram.

5. O-rich and C-rich AGB stars

The AGB stars can be divided into two main spectral classed: oxygen-rich (O-rich or M-type giants) and carbon-rich (C-rich or C-type), depending on the relative abundance of oxygen to carbon in their atmospheres. According to the evolutionary models every star entering the AGB is the O-rich object. During the evolution the dredge-up episodes change the stellar surface chemical composition and turn the star from O-rich into C-rich (Iben and Renzini 1983).

Fig. 2 presents the period–W_I diagrams, separately for stars from the sequences C′, C and D (populated by stars with the Long Secondary Periods). Since the light curves of many variables in our sample show secular variability (sometimes with amplitudes of several magnitudes) and the *I* and *V*-band data span different time baseline, using the mean *I* and *V* luminosities in deriving the W_I index may result in significant errors. Therefore, we derived individual values of W_I for the epochs of our *V*-band points, estimating the *I*-band magnitudes using the closest measurements. Then, we derived the mean W_I by fitting a third order Fourier series to our individual W_I points and integrating the function.

The most conspicuous feature visible in Fig. 2 is the fact that each *PL* sequence splits into two ridges in the $\log P$–W_I plane. The slanted lines were drawn "by hand" to discriminate both groups in each panel:

$$W_I = -7.5 \log P + 25.0,$$

$$W_I = -7.8 \log P + 28.0,$$

$$W_I = -8.6 \log P + 35.2$$

for the sequences C′, C and D, respectively.

Noda *et al.* (2004) used the photometry of the LMC AGB stars originated in the MOA project and plotted the period – (visual) color diagrams separately for each *PL* sequence. They found that the sequences B (corresponding to the merged sequences B and C′ in this paper) and C are split into two groups in this plane. This dichotomy in Miras and SRVs was explained by the coexistence of O-rich and C-rich giants.

This hypothesis can be easily checked by plotting the period–W_I diagram for the spectroscopically confirmed M- and C-type stars. The list of confirmed

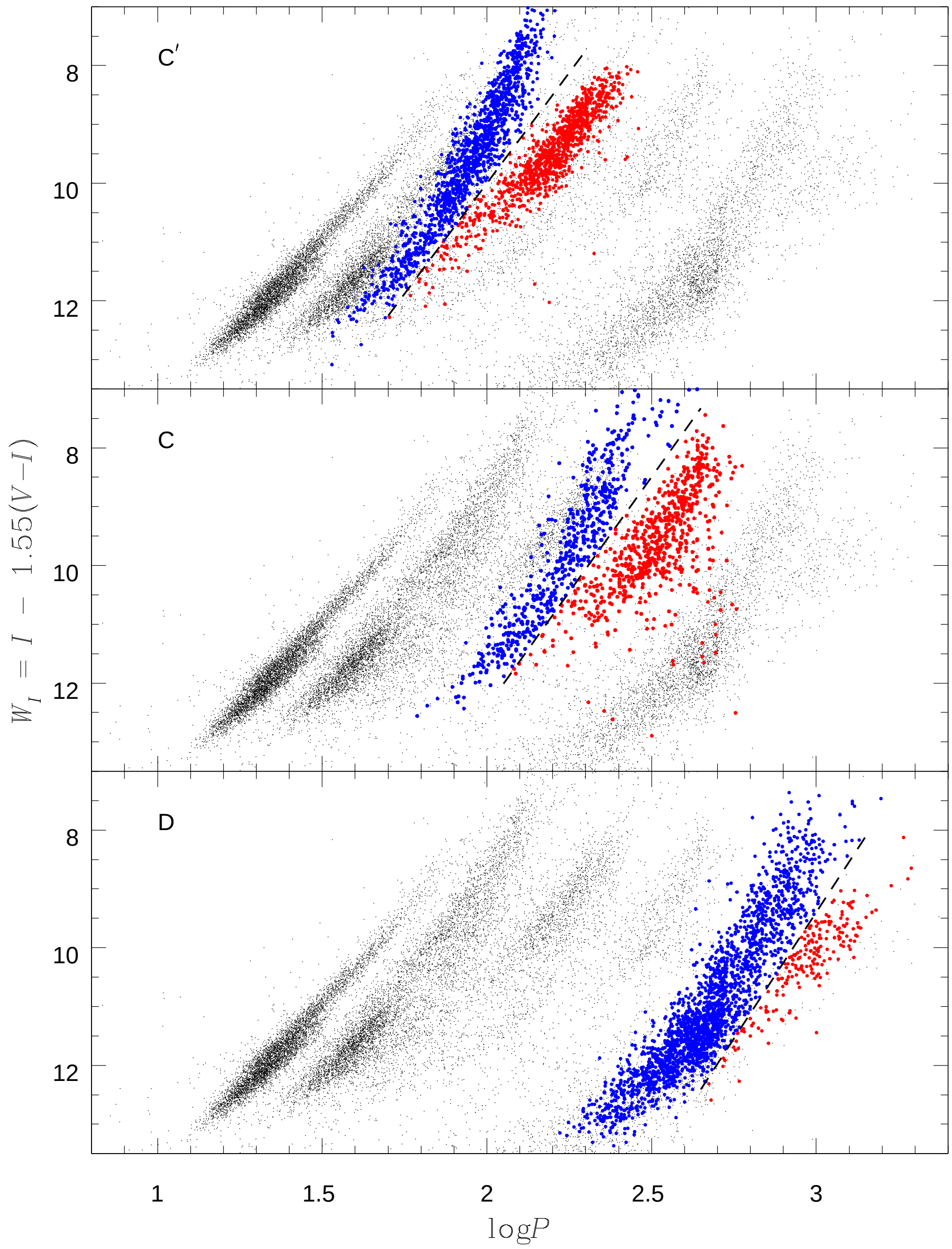

Fig. 2. Period–W_I diagrams for LPVs in the LMC. The color points indicate the stars from the sequences C′ (*upper panel*), C (*middle panel*) and D (*lower panel*). The dashed lines mark the boundaries selected to separate two distinct groups of objects in each panel. Different colors refer to different groups of objects.

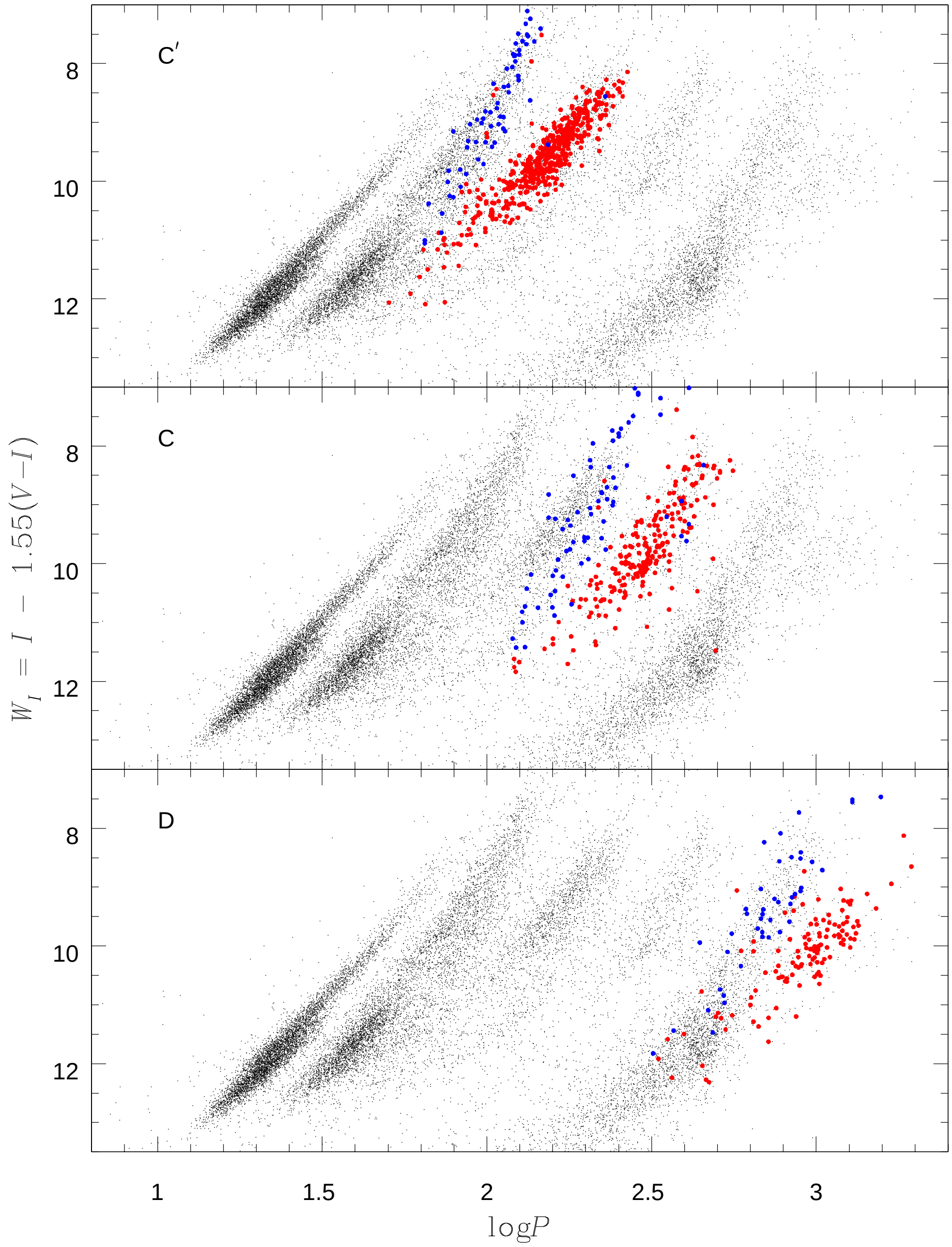

Fig. 3. The same as in Fig. 2, but the color points represent only spectroscopically confirmed O-rich (blue points) and C-rich (red points) AGB stars (Groenewegen 2004).

objects of both spectral classes was compiled by Groenewegen (2004), who identified among the OGLE variables in the LMC 1064 C-rich and 344 O-rich AGB stars. The period–W_I diagrams for these objects are shown in Fig. 3. There is no doubt that the O-rich stars populate the shorter-period ridges, while the C-rich objects fall in the longer-period sequences.

There are several stars of both spectral types which do not follow this rule, *i.e.*, some C-rich giants occupy the shorter-period $\log P$–W_I sequences, and the O-rich giants lie in the longer-period sequences. It can be explained taking into account that some of the stars have an uncertain spectral classification. Groenewegen (2004) showed a number of objects with a different classification in different surveys. He adopted the most recent determination of the spectral type, but the real classification of these objects is, in fact, very uncertain.

Hereby, we provide the method of the discriminating the O- and C-rich LPVs using their V and I magnitudes. Another commonly used photometric method of separating these two populations is the discrimination in the $(J-K_s)$–K_s diagram. O-rich stars are considered to populate colors $(J-K_s) < 1.4$ mag, C-rich stars: 1.4 mag $< (J-K_s) < 2.0$ mag, redder objects are thought to be the AGB stars of both classes surrounded by thick dust shells (Nikolaev and Weinberg 2000). Cioni *et al.* (2005) improved the discrimination criteria using slanted boundary line in the $(J-K_s)$–K_s diagram.

In Fig. 4 we show such color–magnitude diagrams, separately for the sequences C and C′. Blue dots indicate the O-rich objects, while red points show the C-rich giants selected in the period–W_I diagram. As can be expected the M-type objects populate narrow range of $(J-K_s)$ colors, the C-type stars spread over much wider range. However, there is a region occupied by both classes of stars, so the separation of the O-rich and C-rich AGB stars in the NIR color–magnitude diagram can be correct only in the statistical sense, but in the individual cases may be wrong. Our method of distinguishing O- and C-rich Miras and SRVs seem to be more reliable, because in the $\log P$–W_I plane both groups are better separated, especially for brighter objects.

6. Mean K_s-band Magnitudes

The internal scatter of the *PL* sequences in the K_s-band is affected by many factors. When only one random-phase observation per star is available, the *PL* relationship is significantly widened by the amplitude of variability. This effect is particularly noticeable in the sequence C populated by the stars with the largest amplitudes. According to Feast *et al.* (1982) the upper limit for the amplitudes of Miras in the K bandpass is about 1 mag. Thus, the offset in the K magnitude in respect to the mean *PL* relationship for Miras can be as large as 0.5 mag.

To decrease this effect we tried to find a method of converting single epoch K_s-band measurements to the mean magnitudes using the complete I-band light curves. Our estimation is based on shifting phases of the I-band light curves by a constant offset and scaling their amplitudes. This approach assumes that

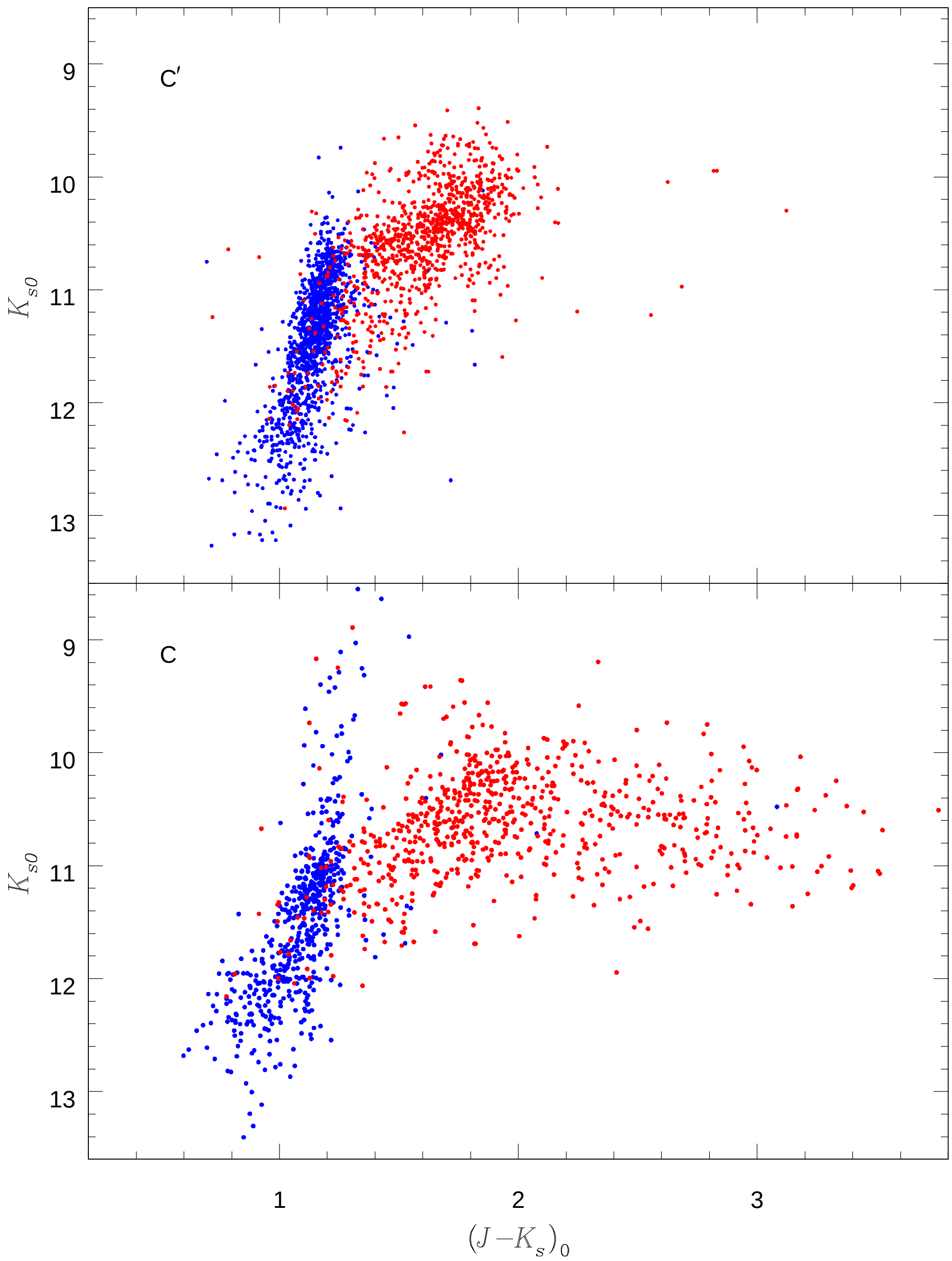

Fig. 4. Color–magnitude $(J - K_s, K_s)$ diagram for stars populating the sequences C′ (*upper panel*) and C (*lower panel*). Blue points represent the O-rich stars, while the red points indicate the C-rich giants.

the shapes of the light curves in different wavebands differ only in amplitudes and phases, what is not true. It is known that Miras in the K_s-band have much more sinusoidal light curves than in the optical part of the spectrum. Thus, our algorithm can recover the mean magnitudes very roughly, but enough to significantly decrease the dispersion of the PL relations.

Because many of the Mira-like variables show secular or very long period variations, we determined the I-band luminosity using unfolded light curves. Whitelock *et al.* (2003) noticed that the amplitudes of these long-term trends depend on the wavelength in roughly the same way as the pulsation amplitudes, *i.e.*, they are smaller at longer wavelengths. For the Julian Date of the K_s observation we added the proper phase lags (see below) and approximated the I-band luminosity for this epoch using three closest points of the light curve. Then, the difference between the obtained luminosity and the mean I-band magnitude were scaled using the $A(K_s)/A(I)$ amplitude ratios, and this value was subtracted from the K_s-band measurement to obtain the mean K_s-band magnitude.

It is known from decades that the NIR maxima of Miras occur with a phase lag of about 0.1 period with respect to the visual light curves (Pettit and Nicholson 1933), but this phenomenon is still rather poorly documented. Recently Smith *et al.* (2005) studied the optical–NIR phase shifts in a number of AGB stars and confirmed that there is a lag between the visual and NIR light curves for Miras, while most of the SRVs do not reveal any detectable phase lags. It is also known that the amplitudes of the giant variability depend on the photometric bandpass, *i.e.*, the amplitudes decrease with the wavelength. Lebzelter and Wood (2005) found the ratio of the K and V amplitudes to be equal to about 0.2.

Since the dependence of the NIR–visual amplitudes and phases is rather poorly known, we decided to estimate the typical amplitude ratios and lag in phases between the I-band and K_s-band light curves for our sample of Miras and SRVs. We used two methods. In the first approach we used two independent K_s-band measurements for each star: one coming from the 2MASS catalog and the other from the 3rd release of the DENIS catalog. The cross-identification of our objects with the DENIS sources was performed in the same manner as in the case of the 2MASS catalog (Section 2). The DENIS K_s-band magnitudes were transformed to the 2MASS system using the equations provided by Carpenter (2001). Then, we tested a range of the phase shifts $(0.0 < \phi_K - \phi_I < 0.2)$ and amplitude ratios $(0.1 < A(K_s)/A(I) < 0.6)$, deriving for each pair of parameters the mean K_s magnitudes independently for the 2MASS and DENIS single epoch measurements. For each star we calculated the difference between the mean luminosities estimated from these two sources, and determined the dispersion of these differences for the whole sample of stars. Finally, we selected the phase offset and the amplitude ratio providing the best agreement between the mean magnitudes estimated using the 2MASS and DENIS measurements.

In the second method we used the 2MASS data only. We chose the $\phi_K - \phi_I$ and $A(K_s)/A(I)$ for which the K_s-band PL relation had the smallest dispersion. We applied both methods separately for four groups of variables: O- and C-

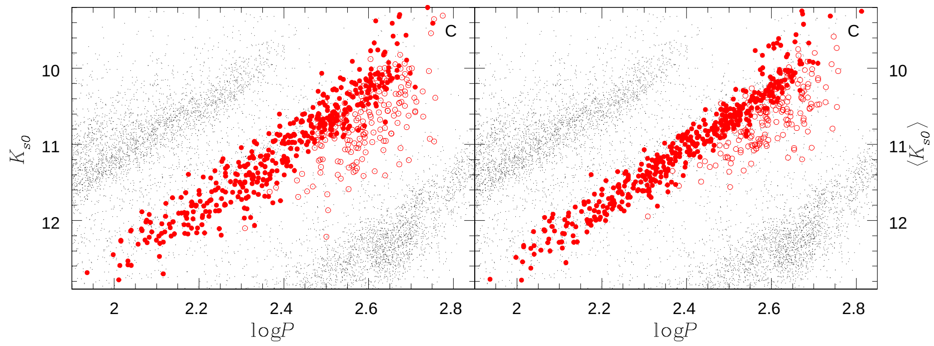

Fig. 5. *Left panel*: the PL sequence C constructed using the single-epoch K_{s0} magnitudes. *Right panel*: the same sequence plotted with the mean magnitudes estimated using the method described in the text. For clarity only the variables with I-band amplitudes exceeding 0.5 mag are plotted. Empty circles indicate the stars with $(J-K_s)>2.3$.

Mira-like stars and O- and C-rich objects from the sequence C′.

The results of these methods appeared to be consistent, and they agree with the previous results. The bulk of both spectral types of stars located in the sequence C reveal the same values of optical–NIR phase lags and amplitude ratios: $\phi_K - \phi_I \approx 0.1$, $A(K_s)/A(I) \approx 0.4$. However, the possible values of the phase shifts in the C-rich Miras seem to cover wider range, from 0.05 to 0.1. The Miras' amplitude ratios agree with the results of Lebzelter and Wood (2005), because the $A(I)/A(V)$ ratio is on average 0.5. For the stars populating the sequence C′ the minimum dispersion shows the lag in phase by about 0.02, but probably in some cases it is somewhat larger, up to 0.05. We found different amplitude ratios for different spectral types: $A(K_s)/A(I) \approx 0.25$ for the O-rich and $A(K_s)/A(I) \approx 0.4$ for the C-rich SRVs in the sequence C′.

The efficiency of our mean K_s-band magnitudes estimation method is demonstrated in Fig. 5. We show here the PL sequence C constructed with the uncorrected single-epoch magnitudes, and the same diagram plotted with the mean K_s magnitudes estimated using our algorithm. For clarity we present only the variables with I-band amplitudes exceeding 0.5 mag, for which the correction is the largest. The improvement of the PL relation is clearly visible.

7. K_s-band PL Relations

We used the mean dereddened K_{s0} luminosities estimated with the procedure described in the previous Section to construct the $PL(K)$ diagram (Fig. 6). The width of the sequences, in particular sequence C, are significantly smaller in comparison with the diagram constructed with uncorrected single-epoch measurements. In Fig. 6 the blue points represent the O-rich stars and the red points mark the C-rich giants, both groups discriminated in the period–W_I diagram.

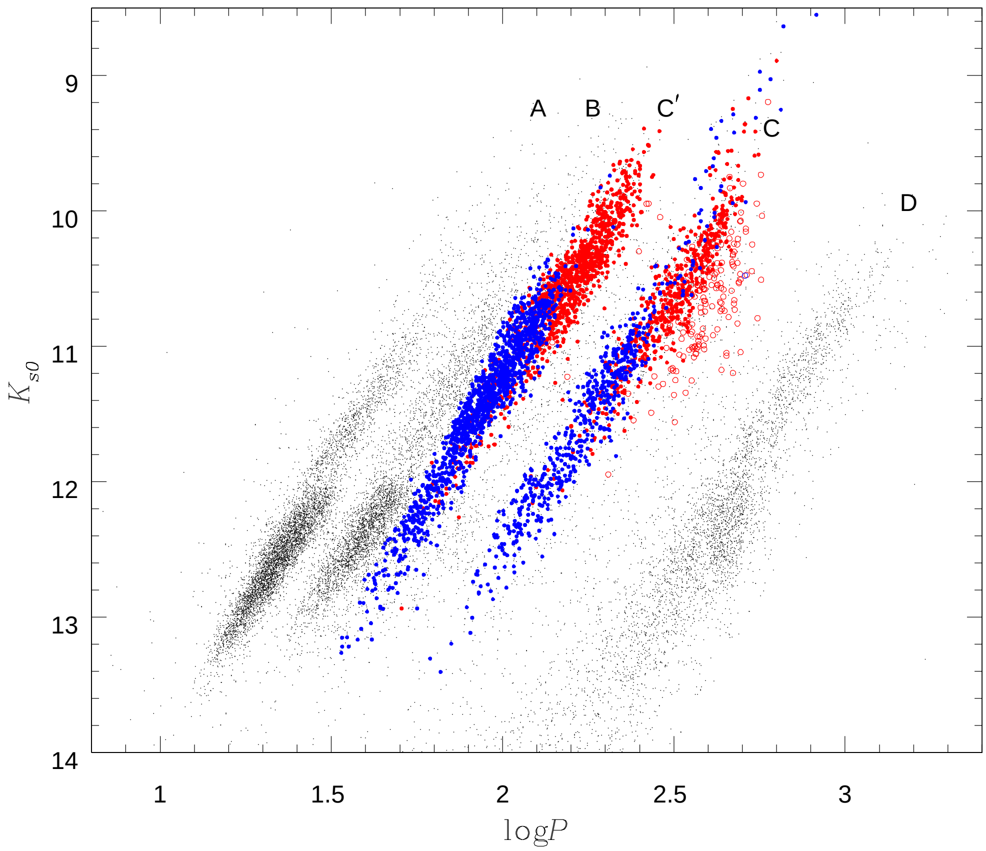

Fig. 6. Period–K_s diagram for Miras and SRVs in the LMC. The blue points show the O-rich variables, while the red points mark the C-rich stars. Empty circles indicate the stars with $(J-K_s)>2.3$ mag, *i.e.*, stars surrounded by dust shells. The single-epoch K_s-band magnitudes of Miras and SRVs were transformed to the mean magnitudes using the procedure described in the text.

Closer look at the $PL(K)$ diagram shows that both spectral types obey different relations between $\log P$ and K_{s0}-band luminosity.

Let us focus on some details seen in Fig. 6. Some brightest Mira-like variables are located above the $PL(K)$ relationship C. Whitelock and Feast (2000) suggested that these objects undergo the hot-bottom burning, but their evolutionary status is unknown. Unfortunately, these stars are close to the saturation limit of the OGLE-II photometry, and they are above this limit in OGLE-III, thus only four years of observations are covered for these stars. Other, shallower photometric surveys (*e.g.*, ASAS, Pojmański 2002) could be useful for studying these objects. Because these variables do not follow the PL sequence of the remaining Mira-like variables, we excluded them from fitting the linear PL relations.

The second feature that can be seen in the PL diagram is the fact that the PL ridge of the C-rich Mira-like variables has considerably larger dispersion than the O-rich sequence. Most of the outliers fall at the right side of the mean PL relation, *i.e.*, they are fainter than the typical C-Miras with the same periods. We checked that the vast majority of the C-rich outliers are very red, with the $(J-K_s)_0 > 2.3$ mag. These objects are marked with empty circles in Fig. 6. We suppose that these stars are highly reddened due to a large amount of circumstellar material around them. The same interpretation of the giants with $(J-K_s) > 2.0$ mag was presented by Nikolaev and Weinberg (2000). These object were also excluded from the fit.

We used the least square method with 2.5σ clipping to fit the K_{s0}-band PL relations separately for M- and C-type stars in the sequences C (with the standard deviation in brackets):

$$\mathrm{O-rich:}\quad K_{s0} = -3.89(\pm 0.05)(\log P - 2.4) + 10.923(\pm 0.011) \quad (\sigma = 0.14)$$

$$\mathrm{C-rich:}\quad K_{s0} = -3.71(\pm 0.05)(\log P - 2.4) + 11.012(\pm 0.008) \quad (\sigma = 0.13)$$

and in the sequence C′:

$$\mathrm{O-rich:}\quad K_{s0} = -4.13(\pm 0.03)(\log P - 2.4) + 9.551(\pm 0.013) \quad (\sigma = 0.13)$$

$$\mathrm{C-rich:}\quad K_{s0} = -3.76(\pm 0.04)(\log P - 2.4) + 9.775(\pm 0.010) \quad (\sigma = 0.15)$$

It can be noticed that the PL relations of the O-rich and C-rich LPVs have different slopes – the C-type stars obey slightly shallower $PL(K)$ relations than the M-giants. The previous works (Feast 1984, Feast *et al.* 1989, Hughes and Wood 1990) suggested the same conclusions, but the uncertainties of the slope determinations were much too large to confirm this effect. Ita *et al.* (2004) used OGLE-II and SIRIUS data to show that the slopes of O- and C-rich LPVs in the sequences C and C′ are different, but the errors of their determinations were only two times smaller than the difference of the slopes. Here, for the first time we show with the reliability larger than 3σ that the slopes of the $PL(K)$ relations for the O-rich LPVs are different than for the C-rich variables.

8. Discussion

Now, it is possible to explain the existence of the additional two sequences found in the $\log P$–W_I diagram by Soszyński *et al.* (2004ab): the sequence C′′ spreading between the sequences C and D, and D′ occupied the region of longer periods than the sequence D. Both ridges are formed by C-type stars: sequence C′′ is populated by Mira-like variables and the sequence D′ by C-rich stars with the Long Secondary Periods. The C-type SRVs from the sequence C′ overlap in the $\log P$–W_I diagram with the M-type Mira-like variables, so this sequence has not been detected earlier.

T a b l e 1

The C/M ratios for stars from the sequences C, C′ and D

	Sequence C	Sequence C′	Sequence D
All	1.21	0.76	–
Above the TRGB	1.64	0.92	0.20

A careful investigation of the *PL* diagrams gives us some clues concerning the nature of the different *PL* relations in the $\log P$–K_s plane. The number of the obscured C-rich Miras (with $(J-K_s)_0 > 2.3$ mag) which do not fit the K_s-band *PL* relation, fall very close to the mean $\log P$–W_{JK} relation. That can be expected, because the Wesenheit index is the reddening independent quantity.

The more surprising feature is that the C-rich and O-rich giants seem to obey the same $\log P$–W_{JK} relations in both, C and C′ sequences. There are two explanations of that fact. First, since the J waveband spectral range of the C-rich AGB stars is strongly affected by the CN and C_2 molecular bands (Cohen *et al.* 1981), the J-band mean luminosities of these objects are on average fainter than the O-rich stars, and the $(J-K_s)$ colors are larger. Thus, in the $\log P$–W_{JK} plane the C-type variables are located relatively higher, and by a coincidence the period–W_{JK} relations of both spectral types are the same.

The second explanation assumes that if the reddening free $\log P$–W_{JK} relations are the same for O-rich and C-rich giants, than the difference between K_s-band *PL* relations of both classes is only an effect of dust obscuration, on average larger in the C-type Miras and SRVs. If the second interpretation is correct, our results paradoxically confirm the idea that un-obscured C- and O-rich Miras fit the same $PL(K)$ relation (Feast *et al.* 1989).

A completely different phenomenon must be responsible for the split of sequences C and C′ in the period–W_I plane. It is known that V-band magnitudes of the M-type LPVs are strongly affected by the titanium oxide (TiO) absorption (Smak 1964, Reid and Goldston 2002). Thus, O-rich stars have larger $(V-I)$ colors than C-rich giants of same K_s-band luminosity, and in consequence they lie higher (for the same periods) in the period–W_I diagram.

Using our method of discriminating the O- and C-rich AGB stars we can derive the relative numbers of C- to M-type AGB stars (C/M ratio). The C/M ratio is considered to be an indicator of the mean metallicity of a stellar population as well as a tracer of the history of star formation (Cioni *et al.* 2005).

The C/M ratios for stars in the sequences C, C′, and D are shown in Table 1. Because the sequence D undoubtedly contains a fraction of first ascent giants, we present also the C/M values for stars above the TRGB ($K_s < 12.05$ mag). It is clear that the largest relative number of C-rich stars occurs in the Mira-like variables, it is intermediate for stars in the sequence C′ and smallest for stars with the Long Secondary Periods. We believe that this is an indicator of the evolutionary status of these groups of AGB stars. The vast majority of variables in the sequence D have secondary periods which falls within the four OSARG *PL* sequences (Soszyński *et al.* 2004a). Thus, our results confirm the fact that the longer the period of the LPVs, the more evolutionary advanced the star is.

It is worth to emphasize that, as can be noticed from Table 1, the C/M ratio depends strongly on the method of the AGB stars selection. Different relative numbers of O- and C-rich stars will be obtained when one considers only Miras, Miras and SRVs, or all AGB stars. Likewise, different C/M ratio will occur when one excludes the stars fainter than the TRGB (the bandpass in which the TRGB is determined also matters) or considers all AGB stars. Therefore, the comparison of the C/M in various environments can be reliable only when the same criteria of the AGB stars selection are fulfilled. This may be the source of large uncertainty in calibration of the C/M *vs.* [Fe/H] relationship.

9. Summary

Based on the OGLE-II and OGLE-III photometry supplemented by the 2MASS NIR data we selected the sample of Miras and SRVs in the LMC. We showed that for these objects the strip pattern of the *PL* distribution is more complex than it was considered before. The sequences C, C$'$ and D split into two separated ridges in the period–W_I plane. This feature can be used for the distinction between the O-rich and C-rich LPVs.

We applied the method of recovering mean K_s magnitudes from single-phase observations and complete *I*-band light curves. The scatter of the K_s-band *PL* sequences, in particular sequence C, considerably decreased in comparison with uncorrected magnitudes. We use these data to show that the K_s-band period–luminosity relations are different for O-rich and C-rich LPVs.

Acknowledgements. We are grateful to Prof. Wojciech Dziembowski and Prof. Bohdan Paczyński for useful comments on this paper. The paper was partly supported by the KBN grant 2P03D02124 to A. Udalski. Partial support to the OGLE project was provided with the NSF grant AST-0204908 and NASA grant NAG5-12212 to B. Paczyński.

This publication makes use of data products from the Two Micron All Sky Survey, which is a joint project of the University of Massachusetts and the Infrared Processing and Analysis Center/California Institute of Technology, funded by the National Aeronautics and Space Administration and the National Science Foundation.

This paper is partly based on DENIS data obtained at the European Southern Observatory.

REFERENCES

Alard, C., and Lupton, R.H. 1998, *Astrophys. J.*, **503**, 325.

Alard, C. 2000, *Astron. Astrophys. Suppl. Ser.*, **144**, 363.

Carpenter, J.M. 2001, *Astron. J.*, **121**, 2851.

Cioni, M.-R.L., Marquette, J.-B., Loup, C., Azzopardi, M., Habing, H.J., Lasserre, T., and Lesquoy, E. 2001, *Astron. Astrophys.*, **377**, 945.

Cioni, M.-R.L., *et al.* 2003, *Astron. Astrophys.*, **406**, 51.

Cioni, M.-R.L., Girardi, L., Marigo, P., and Habing, H.J. 2005, *Astron. Astrophys.*, in press (astro-ph/0509881).

Cohen, J.G., Persson, S.E., Elias, J.H., and Frogel, J.A. 1981, *Astrophys. J.*, **249**, 481.

Cutri, R.M., *et al.* 2003, "2MASS All-Sky Catalog of Point Sources".

Feast, M.W. 1984, *MNRAS*, **211**, 51P.

Feast, M.W., Robertson, B.S.C., Catchpole, R.M., Evans, T.,L., Glass, I.S., and Carter, B.S. 1982, *MNRAS*, **201**, 439.

Feast, M.W., Glass, I.S., Whitelock, P.A., and Catchpole, R.M. 1989, *MNRAS*, **241**, 375.

Fraser, O.J., Hawley, S.L., Cook, K.H., and Keller, S.C. 2005, *Astron. J.*, **129**, 768.

Glass, I.S., and Lloyd Evans, T. 1981, *Nature*, **291**, 303.

Groenewegen, M.A.T. 2004, *Astron. Astrophys.*, **425**, 595.

Hughes, S.M.G., and Wood, P.R. 1990, *Astron. J.*, **99**, 784.

Iben, I. Jr., and Renzini, A. 1983, *Astron. Astrophys. Rev.*, **21**, 271.

Ita, Y., *et al.* 2002, *MNRAS*, **337**, L31.

Ita, Y., *et al.* 2004, *MNRAS*, **347**, 720.

Kiss, L.L., and Bedding, T.R. 2003, *MNRAS*, **343**, L79.

Kholopov, P.N. *et al.* 1985, *General Catalog of Variable Stars, The Fourth Edition*, Nauka, Moscow.

Lebzelter, T., Schultheis, M., and Melchior, A.L. 2002, *Astron. Astrophys.*, **393**, 573.

Lebzelter, T., and Wood, P.R. 2005, *Astron. Astrophys.*, **441**, 1117.

Madore, B.F. 1982, *Astrophys. J.*, **253**, 575.

Nikolaev, S., and Weinberg, M.D. 2000, *Astron. J.*, **542**, 804.

Noda, S., *et al.* 2002, *MNRAS*, **330**, 137.

Noda, S., *et al.* 2004, *MNRAS*, **348**, 1120.

Pettit, E., and Nicholson, S.B. 1933, *Astrophys. J.*, **78**, 320.

Pojmański, G. 2002, *Acta Astron.*, **52**, 397.

Reid, M.J., and Goldston, J.E. 2002, *Astrophys. J.*, **568**, 931.

Schlegel, D.J., Finkbeiner, D.P., and Davis, M. 1998, *Astrophys. J.*, **500**, 525.

Smak, J. 1964, *Astrophys. J. Suppl. Ser.*, **9**, 141.

Smith, B.J., Price, S.D., and Moffett, A.J. 2005, *Astron. J.*, in press (astro-ph/0509204).

Soszyński, I., Udalski, A., Kubiak, M., Szymański, M., Pietrzyński, G., Żebruń, K., Szewczyk, O., and Wyrzykowski, Ł. 2004a, *Acta Astron.*, **54**, 129.

Soszyński, I., Udalski, A., Kubiak, M., Szymański, M., Pietrzyński, G., Żebruń, K., Szewczyk, O., Wyrzykowski, Ł., and Dziembowski, W.A. 2004b, *Acta Astron.*, **54**, 347.

Udalski, A. 2003, *Acta Astron.*, **53**, 291.

Udalski, A., Kubiak, M., and Szymański, M. 1997, *Acta Astron.*, **47**, 319.

Udalski, A., Soszyński, I., Szymański, M., Kubiak, M., Pietrzyński, G., Woźniak, P., and Żebruń, K. 1999, *Acta Astron.*, **49**, 223.

Udalski, A., Szymański, M., Kubiak, M., Pietrzyński, G., Soszyński, I., Woźniak, P., and Żebruń, K. 2000, *Acta Astron.*, **50**, 307.

Whitelock, P.A., and Feast, M.W. 2000, *Mem. Soc. Astr. Ital.*, **71**, 601.

Whitelock, P.A., Feast, M.W., van Loon, J.Th., and Zijlstra, A.A. 2003, *MNRAS*, **342**, 86.

Wood, P.R., and Sebo, K.M. 1996, *MNRAS*, **282**, 958.

Wood, P.R., *et al.* 1999, *in IAU Symp.*, 191, "Asymptotic Giant Branch Stars", Ed. T. Le Bertre, A. Lébre, and C. Waelkens (San Francisco: ASP), 151.

Wood, P.R. 2000, *Publ. Astron. Soc. Aust.*, **17**, 18.

Woźniak, P.R. 2000, *Acta Astron.*, **50**, 421.